Downloaded from UvA-DARE, the institutional repository of the University of Amsterdam (UvA)
http://dare.uva.nl/document/212310

File ID	212310
Filename	Color figures

SOURCE (OR PART OF THE FOLLOWING SOURCE):

Type	Dissertation
Title	Recognition of infection and inflammation in the kidney
Author	K.M. Heutinck
Faculty	Faculty of Medicine
Year	2011
Pages	208
ISBN	978-94-90371-72-2

FULL BIBLIOGRAPHIC DETAILS:
http://dare.uva.nl/record/373821

Copyright

It is not permitted to download or to forward/distribute the text or part of it without the consent of the author(s) and/or copyright holder(s), other than for strictly personal, individual use.

UvA-DARE is a service provided by the library of the University of Amsterdam (http://dare.uva.nl)

COLOR FIGURES

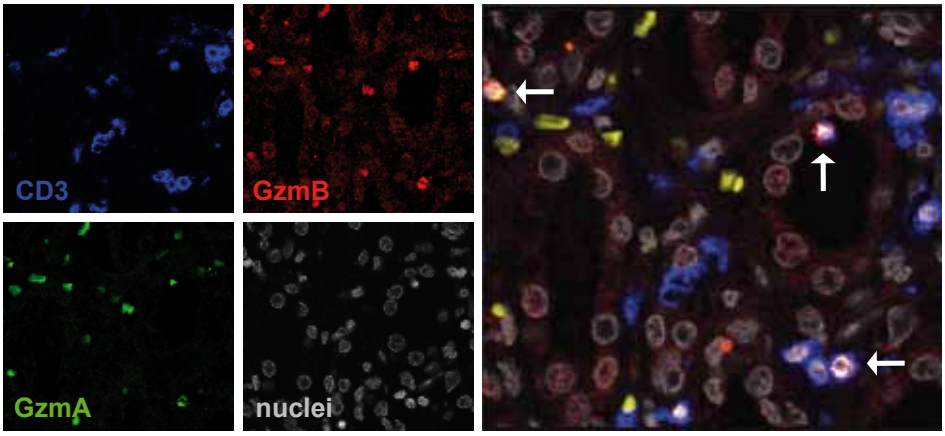

Chapter 3, Figure 3: Expression and co-localization of granzyme A, granzyme B by graft infiltrating T- and NK- cells during rejection. Triple immunohistochemical stainings were performed to identify the source of granzyme A (GzmA) and granzyme B (GzmB) during renal allograft rejection. Depicted is a biopsy with T cell-mediated rejection type 1 showing triple staining with CD3 (blue), GzmA (green), GzmB (red), nuclear counterstaining (grey) and overlay. Many graft infiltrating cells are CD3 positive T-cells containing granzymes, e.g. the triple positive cells located inside a tubulus and in the interstitium (white arrows). Granzyme double positive, CD3 negative cells were also present at a lower frequency, for example the cell at the upper left. The intensity and ratio of GzmA and GzmB differed per cell. For color figure, see appendix.

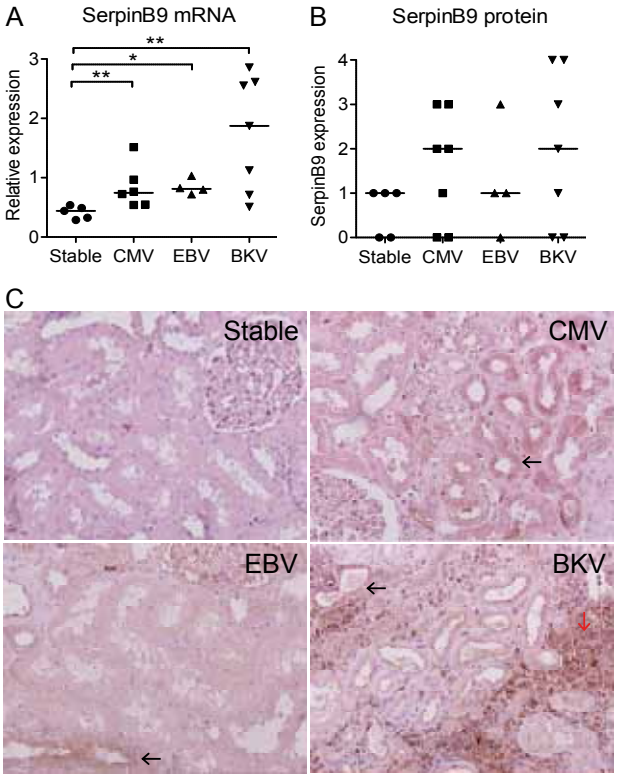

Chapter 4, Figure 5: SerpinB9 expression in the kidney is enhanced during viral infection. A SerpinB9 transcription in frozen biopsy specimens obtained from stable patients (n=5) and patients infected with cytomegalovirus (CMV, n=6), Epstein-Barr virus (EBV, n=4) or BK virus (BKV, n=7) depicted as relative expression (median). **B+C** Immunohostochemical stainings for serpinB9 on formalin-fixed paraffin-embedded tissue slides. **B** Semi-quantitative scoring of the tubular SerpinB9 expression, scored as described in the methods section (median). **C** Representative pictures of the serpinB9 staining pattern observed in stable, CMV, EBV and BKV biopsies, with serpinB9 expression found in the tubuli (black arrows) and infiltrating lymphocytes (red arrow) (magnification 200x). For color figure, see appendix.

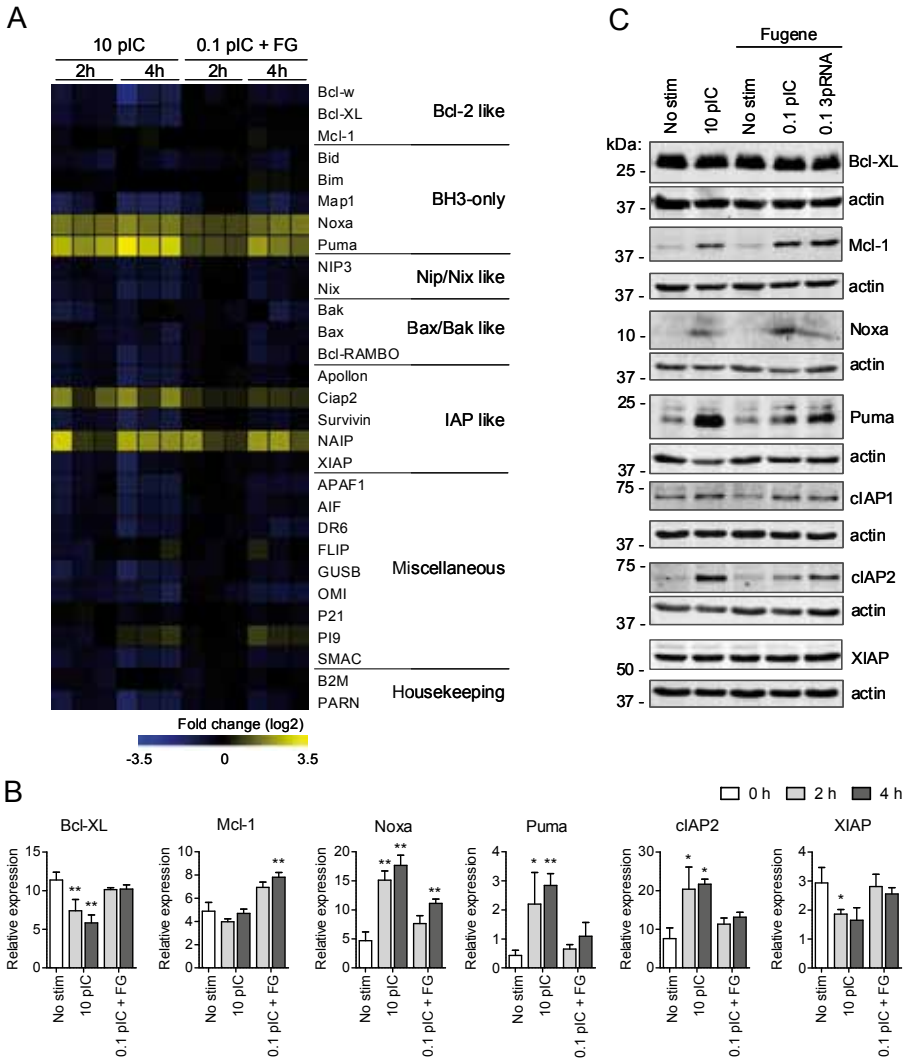

Chapter 5, Figure 3: Activation of dsRNA receptors promotes the expression of pro-apoptotic BH3-only and anti-apoptotic IAP family members. Primary TECs were stimulated with 10 µg/ml poly(I:C) (pIC) or 0.1 µg/ml poly(I:C) and Fugene (pIC + FG) for 2 or 4 h. Subsequently, mRNA expression levels of genes that mediate apoptosis were determined by multiplex ligation-dependent probe amplification (MLPA). **A** Heat-map of fold change (log2) in gene expression compared to unstimulated TECs. Each square represents a single measurement (n=3). Genes that are upregulated are depicted in yellow, genes that are downregulated in blue. **B** Transcription levels of Bcl-XL, Mcl-1, Noxa, Puma, cIAP2 and XIAP measured by MLPA are depicted as relative expression (arbitrary values, mean ± SEM, n≥3). Values were compared to unstimulated cells with paired T-tests. **C** Analysis of pro- and anti-apoptotic genes by Western blot analysis in TECs stimulated for 24 h with 10 µg/ml poly(I:C) (TLR3), 0.1 µg/ml poly(I:C) and Fugene (MDA5), 0.1 µg/ml 3pRNA (RIG-I). Blots are representative for at least three different experiments. For color figure, see appendix.

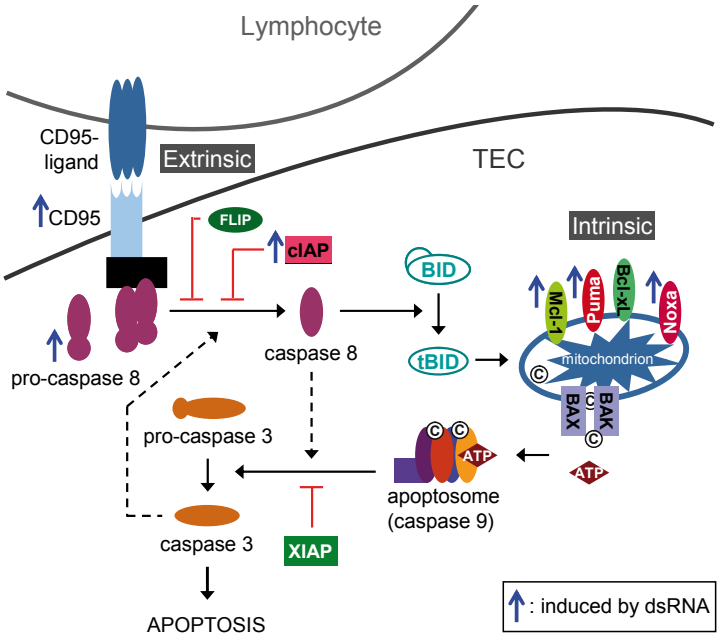

Chapter 5, Figure 5: Model for dsRNA- and CD95-mediated apoptosis in TECs. TECs are type II cells in which death receptor-mediated apoptosis requires activation of the intrinsic apoptosis pathway. CD95/CD95-ligand interaction induces the formation of the death inducing complex (DISC), which includes the adaptor CD95-associated death domain (FADD) and pro-caspase 8 leading to autocleavage of caspase 8. Active caspase 8 can in turn cleave the caspase 8 inhibitor FLICE-like inhibitory protein (FLIP) and BCL-2 interacting domain (BID). The truncated form of BID (tBID) translocates to the mitochondrial membrane where it disrupts the balance between Bcl-2 like proteins like Bcl-XL and Mcl-1 and BH3-only proteins like Noxa and Puma. Anti-apoptotic Bcl-2 like proteins prevent interaction between Bak and Bax, which is essential for mitochondrial outer membrane permeabilization and cytochrome C release. Disruption of mitochondrial integrity leads to the formation of the apoptosome, a protein complex in which caspase 9 is activated in an ATP dependent manner. The apoptosome promotes the activation of effector caspases like caspase 3 leading to cell death. XIAP and cIAP1/2 block apoptosis by inhibiting caspase 3 and 8 activation. We found that expression of these inhibitors prevented death in TECs exposed to a single apoptotic stimulus such as CD95 or dsRNA. Based on these findings we propose that activation of viral dsRNA sensors sensitizes TECs to the attack of CD95-ligand expressing cytotoxic lymphocytes via enhancing the expression of the death receptor CD95, pro-caspase 8, Puma, Noxa and Mcl-1. The effect of dsRNA on expression levels of various mediators of the extrinsic and intrinsic apoptotic pathways are visualized by blue arrows. For color figure, see appendix.

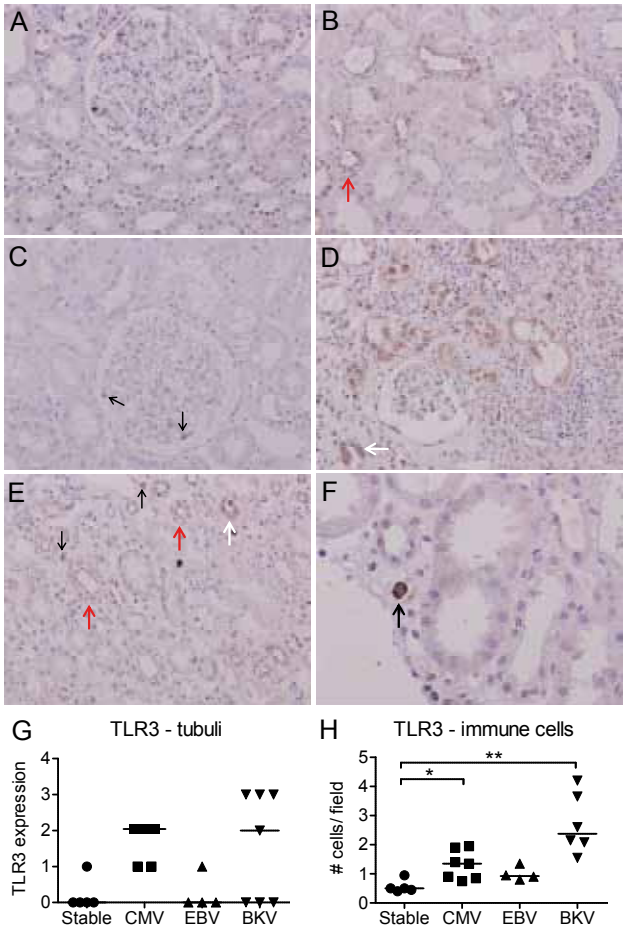

Chapter 6, Figure 2: Tubuli and macrophages express TLR3 during viral infection. Toll-like receptor 3 (TLR3) expression pattern in renal transplant biopsies. Representative pictures of a stable biopsy (**A**) and biopsies obtained during infection with cytomegalovirus (CMV, **B**), Epstein-Barr virus (EBV, **C**) or BK virus (BKV, **D**). **E** Example of TLR3 expression patterns found in renal tubuli, cytoplasmic staining (white arrows) and brush border staining (red arrows). **F** Granular TLR3 staining patterns found in macrophage-like immune cell (black arrows) in the renal interstitium. **G** Semi-quantitative scoring of TLR3 positive tubuli in kidney transplant biopsies from stable patients (n=5) or during infection with CMV (n=6), EBV (n=3) or BKV (n=7) (median). **H** Scoring of the number of TLR3 positive macrophage-like immune cells per field (400x magnification, one data point represent the average of 12 fields). The number of cells during viral infection are compared to the number found in stable biopsies with Mann-Whitney U tests. For color figure, see appendix.

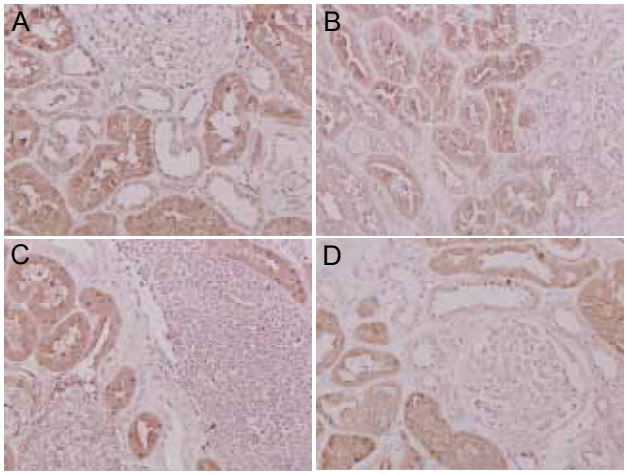

Chapter 6, Figure 3: MDA5 is broadly expressed in the kidney. Melanoma differentiation associated gene 5 (MDA5) expression pattern in renal transplant biopsies. Representative pictures of a stable biopsy (**A**) and biopsies performed during infection with cytomegalovirus (CMV, **B**), Epstein-Barr virus (EBV, **C**) or BK virus (BKV, **D**). For color figure, see appendix.

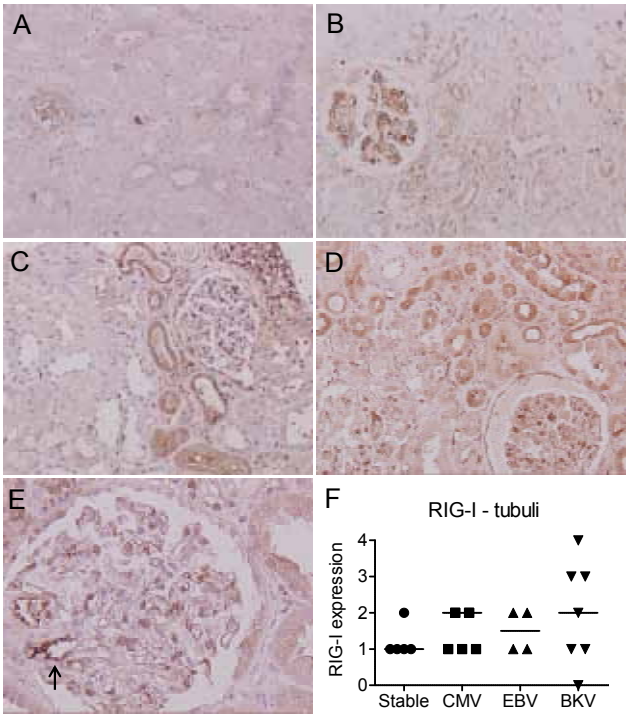

Chapter 6, Figure 4: Tubuli, endothelial cells and kidney infiltrating lymphocytes express RIG-I. Expression pattern of retinoic acid inducible gene-I (RIG-I) in kidney transplant biopsies obtained from stable patients (n=5) or during infection with cytomegalovirus (CMV, n=6), Epstein-Barr virus (EBV, n=4) or BK virus (BKV, n=7). Representative pictures of stable (**A**), CMV (**B**), EBV (**C**) and BKV (**D**) biopsies. **E** Example of RIG-I expression in glomerular capillary (black arrow). **F** Semi-quantitative scoring of RIG-I positive tubuli (median). For color figure, see appendix.